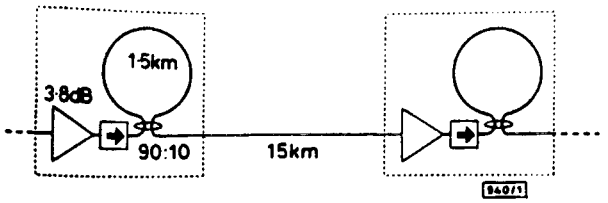

Fig. 1 *Schematic diagram of soliton transmission system including nonlinear optical loop mirrors*

it then becomes very difficult to successfully transmit solitons close to the transmission peak of successive NOLMs. We set the input conditions (N = 1.4 solitons of FWHM 1.5ps) such that the pulses pass through the loop mirrors slightly beyond the peak of the switching curve. This then confers the added advantage that the NOLM provides negative feedback control of the pulse amplitudes. If the pulse energy fluctuates upwards, then the NOLM transmittivity decreases, restoring the pulse towards its original state, and vice versa.

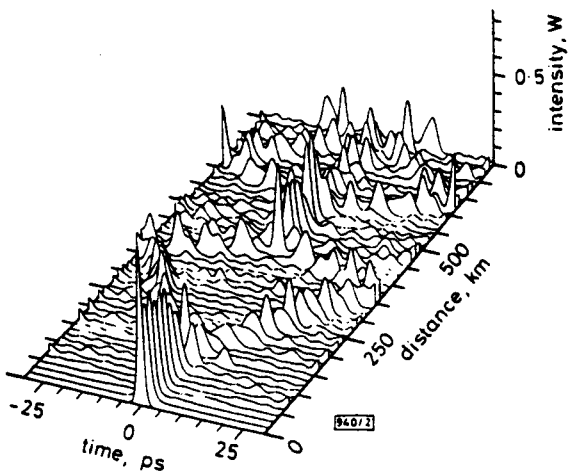

Fig. 2 *Propagation of 1.5ps FWHM soliton through amplifiers spaced at 15km intervals, without use of NOLM filtering*

The effectiveness of our scheme is demonstrated by the results of numerical simulations shown in Figs. 2 and 3. Without the loop mirrors, a 1.5ps soliton injected into the chain of amplifiers rapidly disintegrates after 100km. By contrast Fig. 3 shows minimal temporal distortion when the loop mirrors are included. To completely describe the propagation of such short pulses in optical fibre, consideration must be made of stimulated Raman scattering, which has been neglected in the results presented above. When this is included, we have found that the pulse's central frequency shifts by 0.8THz over the system span. The energy of each pulse at the amplifier outputs is 2.4pJ, which if translated into a 100GHz bit stream (equal ones and zeros) would imply a mean power of 120mW. Practical implementation of this will be dependent on improvements in optical amplifier technology.

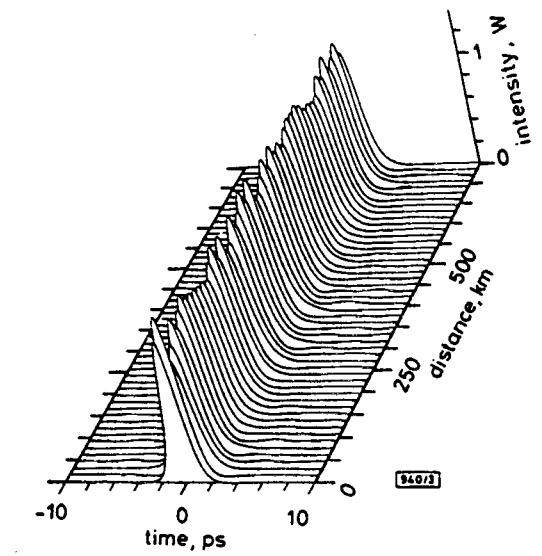

Fig. 3 *Propagation of 1.5ps solitons through amplifiers spaced at 15km interval, each amplifier followed by loop mirror filter*

In conclusion, we have devised a new method of propagating 1.5ps optical solitons over 750km using optical amplifiers spaced 15km apart by using all fibre nonlinear optical loop mirrors. This simple passive control of the solitons allows access to a transmission regime which has previously been considered wholly impractical. The result provides impetus to the study of short pulse communications, with the ultimate goal of achieving operation in the region of 100Gbit/s.

Acknowledgment: This work was supported by SERC.

26 April 1994
Electronics Letters Online No: 19940716

N. J. Smith and N. J. Doran (*Dept. Electronic Engineering & Applied Physics Aston University, Aston Triangle, Birmingham B4 7ET, United Kingdom*)

References

1 DORAN, N.J.: 'Nonlinear fibre devices and soliton communications', *in* OSTROWSKY, D.B., and REINISCH, R. (Eds.): 'Guided wave nonlinear optics: Proceedings of the NATO advanced study institute on guided wave nonlinear optics', Càrgese, France, August 12-21st, 1991' (Kluwer Academic Publishers, Dortrecht, The Netherlands, 1992)

2 BLOW, K. J., and DORAN, N. J.: 'Average soliton dynamics and the operation of soliton systems with lumped amplifiers', *IEEE Photonics Technol. Lett.*, 1991, **3**, pp. 369–371

3 NAKAZAWA, M., and KUROKAWA, K.: 'Femtosecond soliton transmission in 18 km long dispersion shifted distributed erbium-doped fibre amplifier', *Electron. Lett.*, 1991, **27**, (15), pp. 1369–1371

4 GORDON, J. P.: 'Dispersive perturbations of solitons of the nonlinear Schrödinger equation', *J. Opt. Soc. Am., B*, 1992, **9**, (1), pp. 91–97

5 SMITH, N. J., BLOW, K. J., and ANDONOVIC, I.: 'Sideband generation through perturbations to the average soliton model', *J. Lightwave Technol.*, 1992, **LT-10**, (10), pp. 1329–1333

6 DORAN, N. J., and WOOD, D.: 'Non linear optical loop mirror', *Opt. Lett.*, 1988, **13**, (1), pp. 56–58

7 DULING, I. N.: 'All-fiber ring soliton laser mode locked with a nonlinear mirror', *Opt. Lett.*, 1991, **16**, (8), pp. 539–541

8 KODAMA, Y., ROMAGNOLI, H., and WABNITZ, S.: 'Soliton stability and interactions in fibre lasers', *Electron. Lett.*, 1992, **28**, (21), pp. 1981–1983

9 MATSUMOTO, M., IKEDA, H., and HASEGAWA, A.: 'Suppression of noise accumulation in bandwidth limited soliton transmission by means of nonlinear loop mirrors', *Opt. Lett.*, 1994, **19**, (3), pp. 183–185

843.

Discrimination between strain and temperature effects using dual-wavelength fibre grating sensors

M. G. Xu, J.-L. Archambault, L. Reekie and J. P. Dakin

Indexing terms: Gratings in fibres, Fibre optic sensors

The spectral behaviour of two superimposed fibre gratings having different Bragg wavelengths (850 and 1300nm) with respect to strain and temperature has been studied. The results show that the ratio of sensitivity at two Bragg wavelengths is dependent on strain and temperature, which can be used for simultaneous measurement of these parameters using a single sensing element.

Introduction: Considerable research effort has been devoted to fibre Bragg grating sensors, which are particularly well suited to measuring strain in smart structures [1]. However, undesirable temperature sensitivity of fibre grating sensors may complicate their application as strain gauges. On a single measurement of the Bragg wavelength shift, it is impossible to differentiate between the effects of changes in strain and temperature. Various schemes for discriminating between these effects have been developed. These include using a second grating element contained within a

different material and placed in series with the first grating element [2] and the use of a pair of fibre gratings surface-mounted on the opposite surface of a bent mechanical structure [3]. However, these methods have limitations when it is desired to interrogate the wavelength of a large number of fibre gratings. Other schemes, such as measuring two different wavelengths or two different optical modes [4, 5], and the use of dispersive Fourier transform spectroscopy [6], have been employed in interferometric and polarimetric fibre optic sensors. Therefore, to resolve these two effects in fibre grating sensors, it is logical to measure two different Bragg wavelengths, and the use of two superimposed fibre gratings seems to be a suitable option. Nevertheless, little is known about the ratio of sensitivity at two Bragg wavelengths with relation to strain and temperature. It is important to understand this dependence, and in this Letter we present the initial results of our recent studies into this effect.

Principle: Assuming that the strain- and thermally-induced perturbations are linear, the Bragg wavelength changes $\Delta\lambda_\varepsilon$ and $\Delta\lambda_T$, in response to a strain change $\Delta\varepsilon$ and temperature change ΔT, can be expressed in the form

$$\Delta\lambda_\varepsilon = K_\varepsilon \Delta\varepsilon$$
$$\Delta\lambda_T = K_T \Delta T \qquad (1)$$

where $K\varepsilon = \partial\lambda/\partial\varepsilon$ is related to the Poisson ratio of the fibre, the photoelastic coefficient, and the effective refractive index of the fibre core. $K_T = \partial\lambda/\partial T$ is determined by the thermal expansion coefficient and the thermo-optic coefficient. As the photoelastic and thermo-optic coefficients are wavelength dependent, fractional wavelength changes of each of the two superimposed gratings will be different although each grating is subject to the same level of strain. In other words, this suggests a method for simultaneously measuring strain and temperature, or compensating for the temperature during strain measurement. In general, the change in Bragg wavelength of the fibre grating $\Delta\lambda_B$, due to a combination of strain and temperature, can be expressed as

$$\Delta\lambda_B(\varepsilon, T) = K_\varepsilon \Delta\varepsilon + K_T \Delta T \qquad (2)$$

This assumes that the strain and thermal response are essentially independent, i.e. the related strain-temperature cross-term is negligible, a behaviour which has already been found to apply well for small perturbations [1]. As a result, for the two Bragg wavelengths to be measured, the following relation holds:

$$\begin{pmatrix} \Delta\lambda_{B1} \\ \Delta\lambda_{B2} \end{pmatrix} = \begin{pmatrix} K_{\varepsilon 1} & K_{T1} \\ K_{\varepsilon 2} & K_{T2} \end{pmatrix} \begin{pmatrix} \Delta\varepsilon \\ \Delta T \end{pmatrix} \qquad (3)$$

where 1 and 2 refer to the two wavelengths: 1300 and 850nm, respectively. The elements of the **K** matrix can be determined experimentally by separately measuring the Bragg wavelength changes with strain and temperature. Once **K** is known, changes in both strain and temperature can be determined using the inverse of eqn. 3 provided that the matrix inversion is well-conditioned.

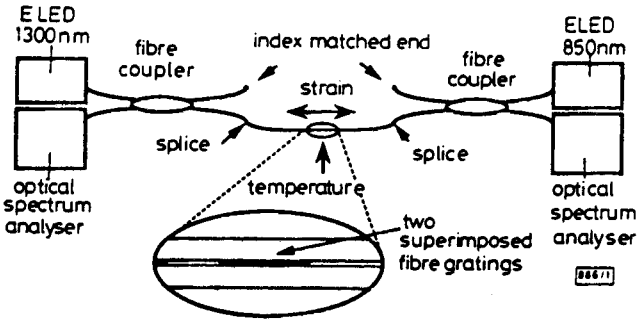

Fig. 1 *Schematic diagram of experiment arrangement*

Experiment and discussion: The key sensing elements are the superimposed fibre gratings, with nominal Bragg wavelengths of ~1298 and ~848nm, peak reflectivities of ~70 and ~55%, and optical bandwidths of ~0.9 and ~0.45nm (FWHM), respectively. The experiment is shown in Fig. 1. Light from the 850 and 1300nm ELEDs, of bandwidth (FWHM) ~56nm, was split via two corresponding fibre couplers to the gratings and the light reflected from the two fibre gratings was monitored using a commercial optical spectrum analyser (Ando AQ-6310B).

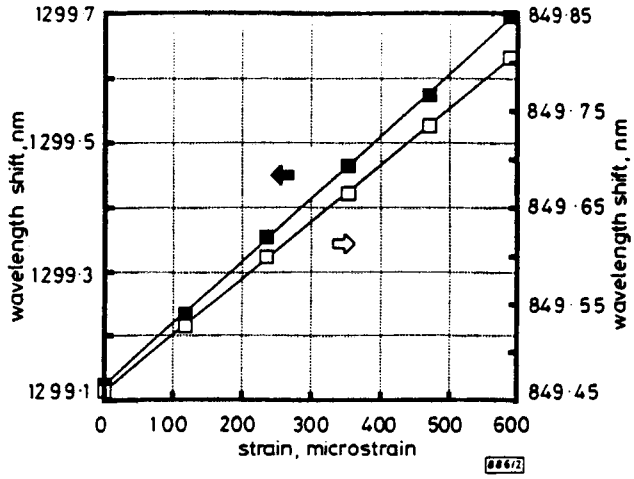

Fig. 2 *Strain-induced wavelength shift at two Bragg wavelengths*

□ measurements at 850nm
■ measurements at 1300nm
—— linear fit

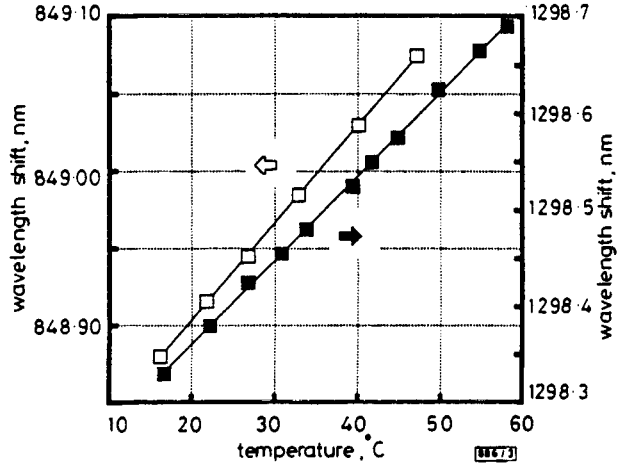

Fig. 3 *Thermally-induced wavelength shift at two Bragg wavelengths*

Strain was applied using a micrometer driven stage and temperature was accurately set by using a Peltier heat pump regulated by a thermoelectric temperature controller. The strain coefficients were measured while the fibre gratings were kept at a constant temperature of 24.8°C to avoid errors resulting from temperature changes. However, the fibre gratings were held unstrained during the thermal coefficient measurement. For convenience of demonstrating the concept, the four elements of the **K** matrix were obtained by separately measuring the Bragg wavelength of each fibre grating for changes in strain only and subsequently for changes in temperature only. Linear regression analysis gave correlation coefficients of ≥ 0.998 for all four relationships for a strain range of 0–600 μstrain and a temperature range of 10–60°C, as shown in Figs. 2 and 3. The measured values of the **K** elements were

$$K_{\varepsilon 1} = 0.96 \pm 6.5 \times 10^{-3} \text{ pm}/\mu\text{strain}$$
$$K_{\varepsilon 2} = 0.59 \pm 3.4 \times 10^{-3} \text{ pm}/\mu\text{strain}$$
$$K_{T1} = 8.72 \pm 7.7 \times 10^{-2} \text{ pm}/°\text{C}$$
$$K_{T2} = 6.30 \pm 3.7 \times 10^{-2} \text{ pm}/°\text{C}$$

which gives a nonzero determinant of **K** with a standard error of 7.4%, thus the matrix is well-conditioned.

If the inverse matrix is used to predict strain and temperature from the wavelength measurements, errors of typically 10 μstrain and ±5°C are observed for the measurement range of 600 μstrain and 50°C. Possible causes of these errors are: the creep between the glue and fibre coating at bonding points, accuracy of the micrometer driven stage, and the limited resolution of the spectrum analyser and strain and temperature measurement range. Using a more accurate interrogation system, which is currently under development, we would expect to improve the matrix conditioning and thus achieve higher resolution for the wavelength measurement.

Conclusion: We have demonstrated the feasibility of simultaneous measurement of strain and temperature using two superimposed fibre gratings. Work is being directed towards extending the strain and temperature measurement range and improving the measurement resolution using a more accurate interrogation system.

Acknowledgments: The ORC is a UK government funded (SERC) Interdisciplinary Research Centre.

21 April 1994
Electronics Letters Online No: 19940746

M.G. Xu, J.-L. Archambault, L. Reekie and J.P. Dakin
(Optoelectronics Research Centre, University of Southampton, Southampton SO17 1BJ, United Kingdom)

References

1 MOREY, W. W., MELTZ, G., and GLENN, W. H.: 'Fibre optic Bragg grating sensors'. Proc. SPIE, 1989, **1169**, pp. 98–107
2 MOREY, W. W., MELTZ, G., and WELSS, J. M.: 'Evaluation of a fiber Bragg grating hydrostatic pressure sensor'. Proc. OFS'8, 1992, Monterey, USA, Postdeadline Paper PD-4.4
3 XU, M. G., ARCHAMBAULT, J.-L., REEKIE, L., and DAKIN, J. P.: 'Thermally-compensated bending gauge using surface-mounted fibre gratings', to be published in *Int. J. Optoelectron.*
4 FARAHI, F., WEBB, D. J., JONES, J. D. C., and JACKSON, D. A.: 'Simultaneous measurement of temperature and strain: cross-sensitivity considerations', *J. Lightwave Technol.*, 1990, **LT-18**, pp. 138–142
5 CULSHAW, B., and MICHIE, C.: 'Fibre optic strain and temperature measurement in composite materials – A review of the OSTIC programme'. Proc. Int. Symp. on Advanced materials for lightwave structures, ESTEC, Noordwijk, The Netherlands, 1992, pp. 393–398
6 FLAVIN, D. A., MCBRIDE, R., and JONES, J. D. C.: 'Simultaneous measurement of temperature and strain by dispersive Fourier transform spectroscopy'. Proc. OFS'93, 1993, Florence, Italy, pp. 333–336

Method for finding true North using a fibre-optic gyroscope

R.B. Dyott

Indexing term: Fibre optic gyroscopes

True North is found by positioning a fibre-optic gyroscope with its coil axis in the horizontal plane and taking readings of the signal due to the Earth's rotation. Accuracies of ~ 7min of arc standard deviation are obtained.

Introduction: In a recent report on the use of the fibre optic gyroscope to find North, the plane of the sensing coil is rotated about a vertical axis through 360° at 24 equal angular increments and the resultant variation of the gyroscope output fitted to a sinusoidal curve [1]. The method described here uses an alternative scheme, with four or five azimuthal points and no sinusoidal matching, which shortens the procedure considerably.

Principle of operation: The gyroscope (gyro) is positioned with its axis in the horizontal plane and pointing successively in three arbitrary directions. From the gyro outputs at the three directions the angle between any of the directions and true North can be determined.

Let the angle between the first direction and the North-South line be θ. The gyro output S_1 can then be written as

$$S_1 = a\cos\theta + k \tag{1}$$

where a is a constant of proportionality and k is a residual or background independent of direction. Both a and k are assumed, for the moment, to be constant with time. Moving the gyro axis by angle θ_1 to point in a second direction gives an output

$$S_2 = a\cos(\theta + \Phi_1) + k \tag{2}$$

Moving to a third direction through a different angle Φ_2 gives

$$S_3 = a\cos(\theta + \Phi_2) + k \tag{3}$$

Then

$$S_1 - S_2 = a[\cos(\theta) - \cos(\theta + \Phi_1)] \tag{4}$$

$$S_1 - S_3 = a[\cos(\theta) - \cos(\theta + \Phi_2)] \tag{5}$$

and

$$\frac{S_1 - S_2}{S_1 - S_3} = \frac{\cos(\theta) - \cos(\theta + \Phi_1)}{\cos(\theta) - \cos(\theta + \Phi_2)} \tag{6}$$

Because Φ_1 and Φ_2 are known, θ can be found by iteration.

(i) *Particular case:* If Φ_1 and Φ_2 are made to be $+\pi/2$ and $-\pi/2$, then

$$\frac{S_1 - S_2}{S_1 - S_3} = \frac{\cos(\theta) - \cos(\frac{\pi}{2} + \theta)}{\cos(\theta) - \cos(\frac{\pi}{2} - \theta)} = \frac{\cos(\theta) + \sin(\theta)}{\cos(\theta) - \sin(\theta)} \tag{7}$$

(ii) *Optimum point of operation:* Put

$$P = \frac{S_1 - S_2}{S_1 - S_3} = \frac{\cos(\theta) + \sin(\theta)}{\cos(\theta) - \sin(\theta)} \tag{8}$$

then

$$\frac{dP}{d\theta} = -\left[1 + \left(\frac{\cos(\theta) + \sin(\theta)}{\cos(\theta) - \sin(\theta)}\right)^2\right] = -(1 + P^2)$$

At the point of inflection $d^2P/d\theta^2 = 0$

$$\frac{d^2P}{d\theta^2} = -2P\frac{dP}{d\theta} = 2P(1 + P^2) = 0 \tag{9}$$

If $1 + P^2 = 0$, $P^2 = -1$, P is imaginary. If $P = 0$, $\theta = \pi/4$ and $dP/d\theta$ is maximum. Therefore, for the region of maximum sensitivity the initial direction should be set at approximately 45° to the North-South direction.

(iii) *Estimate of accuracy:* Because, with orthogonal directions, S_1, S_2 and S_3 can never all be of the same polarity, then if S_1 is positive and S_2 is positive, S_3 will be negative. Then ideally at 45°

$$P = \frac{0}{2S_1} \tag{10}$$

However, owing to the noise equivalent rotation rate $\Delta\Omega$ giving a noise signal ΔS, there will be a residual

$$\Delta P = \frac{\Delta S}{2(S_1 + \Delta S)} \simeq \frac{\Delta S}{2S_1} \tag{11}$$

The gyro gives maximum signal when its axis is aligned North/South; then

$$S_{max} \propto \Omega_e \cos(latitude)$$

where Ω_e is the Earth's rotation rate (15.041°/h = 7.292 × 10^{-5}rad/s).

$$S_1 = S_{max}\cos\left(\frac{\pi}{4}\right) = \frac{S_{max}}{\sqrt{2}} \tag{12}$$

and

$$\frac{\Delta S}{2S_1} = \frac{\Delta S}{\sqrt{2}S_{max}} = \frac{\Delta\Omega}{\sqrt{2}\Omega_e\cos(latitude)} \tag{13}$$

Because

$$\frac{dP}{d\theta} = -(1 + P^2) \tag{14}$$

$$\Delta\theta = -\frac{\Delta P}{(1 + P^2)} \tag{15}$$

at $\theta = \pi/4$, $P = 0$ so that

$$\Delta\theta = angle\ error = \frac{\Delta\Omega}{\sqrt{2}\Omega_e\cos(latitude)} \tag{16}$$

The accuracy improves as the square root of the integration time. There is, however, a limit imposed by the gyro drift. Suppose the drift is Ω_D°/h and the noise equivalent rotation rate is $\Delta\Omega$°/h/$\sqrt{(H_Z)}$ = Ω_N°/√h, then for both errors to be equal $\Omega_N/\sqrt{t} = \Omega_D t$ where t is the integration time in hours; then $t^{3/2} = \Omega_N/\Omega_D$, and the optimum integration time is